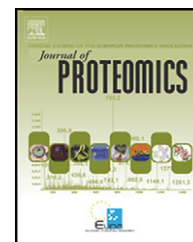


Available online at www.sciencedirect.com

SciVerse ScienceDirect

www.elsevier.com/locate/jprot

Hemopexin is up-regulated in plasma from type 1 diabetes mellitus patients: Role of glucose-induced ROS

Chia-Ching Chen^{a,1}, Ying-Chieh Lu^{b,1}, Yi-Wen Chen^{b,1}, Wen-Li Lee^a, Chieh-Hsiang Lu^c, You-Hsuan Chen^b, Yun-Ching Lee^b, Szu-Ting Lin^b, John F. Timms^{d,*}, Ying-Ray Lee^{e,f,*}, Hsiu-Chuan Chou^{g,*}, Hong-Lin Chan^{b,**}

^aDepartment of Pediatrics, Chiayi Christian Hospital, Chiayi, Taiwan

^bInstitute of Bioinformatics and Structural Biology and Department of Medical Science, National Tsing Hua University, Hsinchu, Taiwan

^cDivision of Endocrinology and Metabolism, Department of Internal Medicine, Chiayi Chirsitan Hospital, Chiayi, Taiwan

^dEGA Institute for Women's Health, University College London, London, UK

^eDepartment of Medical Research, Chiayi Chirsitan Hospital, Chiayi, Taiwan

^fMin-Hwei College of Health Care Management, Tainan, Taiwan

^gDepartment of Applied Science, National Hsinchu University of Education, Hsinchu, Taiwan

ARTICLE INFO

Article history:

Received 23 February 2012

Accepted 29 April 2012

Keywords:

Type 1 diabetes mellitus

2D-DIGE

MALDI-TOF mass spectrometry

Reactive oxygen species

Hemopexin

ABSTRACT

Type 1 diabetes mellitus (T1DM) is an insulin-dependent metabolic disease in the world and often occurs in children and adolescents. Recent advances in quantitative proteomics offer potential for the discovery of plasma proteins as biomarkers for tracking disease progression and for understanding the molecular mechanisms of diabetes. Comparative proteomic analysis of the plasma proteomes from T1DM cases and healthy donors with lysine- and cysteine-labeling 2D-DIGE combining MALDI-TOF/TOF mass spectrometry revealed that 39 identified T1DM-associated plasma proteins showed significant changes in protein expression including hemopexin, and 41 in thiol reactivity. Further study showed that hemopexin can be induced in numerous cell lines by increasing the glucose concentration in the medium. Interestingly, glucose-induced hemopexin expression can be reduced by reactive oxygen species (ROS) scavengers such as glutathione, implying that hemopexin expression is linked to glucose-induced oxidative stress. In conclusion, the current work has identified potential T1DM biomarkers and one of these, hemopexin, can be modulated by glucose through a ROS-dependent mechanism.

© 2012 Elsevier B.V. All rights reserved.

Abbreviations: 2-DE, two-dimensional gel electrophoresis; CCB, colloidal Coomassie Blue; CHAPS, 3-[[3-(cholamidopropyl)-dimethylammonio]-1-propanesulfonate]; ddH₂O, double deionized water; DIGE, differential gel electrophoresis; DTT, dithiothreitol; MALDI-TOF MS, matrix assisted laser desorption ionization-time of flight mass spectrometry; ROS, reactive oxygen species; T1DM, type 1 diabetes mellitus.; TFA, trifluoroacetic acid; T1DM, type 1 diabetes mellitus

* Corresponding authors.

** Correspondence to: H.-L. Chan, Institute of Bioinformatics and Structural Biology and Department of Medical Science, National Tsing Hua University, Hsinchu, Taiwan.

E-mail addresses: john.timms@ucl.ac.uk (J.F. Timms), yingray.lee@gmail.com (Y.-R. Lee), chouhc@mail.nhcue.edu.tw (H.-C. Chou), hlchan@life.nthu.edu.tw (H.-L. Chan).

¹ These authors contributed equally to this work.

1874-3919/\$ – see front matter © 2012 Elsevier B.V. All rights reserved.

doi:10.1016/j.jprot.2012.04.047

Please cite this article as: Chen C-C, et al, Hemopexin is up-regulated in plasma from type 1 diabetes mellitus patients: Role of glucose-induced ROS, J Prot (2012), doi:10.1016/j.jprot.2012.04.047

1. Introduction

Type 1 diabetes mellitus (T1DM) is an insulin-dependent metabolic disease in the world and often occurs in children and adolescents. According to Finne's report, approximately 8% of type 1 diabetic patients developed end-stage of nephropathy through subclinical stage, microalbuminuria, and macroalbuminuria [1,2]. Although urinary albumin is a clinical indicator of the disease, only a small portion of patients with microalbuminuria progress to end-stage nephropathy. Thus, better biomarkers are required to monitor the progression of type 1 diabetes mellitus and the response to therapies.

Serum or plasma is the preferred specimen for biomarker discovery and testing due to its ease of availability and its potential richness in biological information related to multiple physiological disorders. Accordingly, numerous studies have been made to identify biomarkers to monitor the progression of type 1 diabetes mellitus [3,4]. However, most studies have concentrated on genomic profiling approaches as well as animal model-based experiments, with relatively low correlation in response to the clinical prognosis and diagnosis of type 1 diabetes mellitus through human plasma samples [5,6]. Recent studies also indicated that hyperglycemia might induce the overproduction of superoxide by the electrontransport chain in mitochondria [7]. Moreover, this oxidative stress might potentially induce post-translational modifications of proteins leading to the alteration of their functions and the pathogenic processes of diabetic complications [8,9]. Although the major targets of oxidative stress have been shown to be the cysteines and methionines [10], no report demonstrates the globally plasma protein targets of oxidative stress in type 1 diabetes mellitus in our knowledge.

Proteomics is a powerful tool to monitor protein expression changes in response to drug treatment. 2-DE remains an important technique in proteomics for global protein profiling within biological samples and plays a complementary role to LC-MS-based analysis [11]. However, reliable quantitative comparison between gels remains the primary challenge in 2-DE analysis. A significant improvement in gel-based protein detection and quantification was achieved by the introduction of 2D-DIGE, where numerous samples can be co-detected on the same gel using differential fluorescent labeling. This approach alleviates gel-to-gel variation and allows comparison of the relative amount of resolved proteins across different gels using a fluorescently-labeled internal standard. Moreover, the 2D-DIGE technique has the advantages of a broader dynamic range of detection, higher sensitivity and greater reproducibility than traditional 2-DE [11]. This innovative technology relies on the pre-labeling of protein samples on the amino group of lysine residues with fluorescent dyes (Cy2, Cy3 and Cy5) before electrophoresis. Each dye has a distinct fluorescent wavelength, allowing pairs of experimental samples and an internal standard to be simultaneously separated in the same gel. The internal standard, which is a pool of an equal amount of all samples, helps to provide accurate normalization and spot matching and increases statistical confidence in relative quantification across gels [12–18]. More recently, a cysteine labeling version of 2D-DIGE was developed, using ICy dyes (iodoacetyl cyanine dyes) which react with the free thiol group of cysteines via alkylation.

The pair of ICy dyes (ICy3 and ICy5) have been used to monitor redox-dependent protein thiol modifications in a model cell system exposed to hydrogen peroxide and in plasma fractions exposed to UVC [19,20].

In order to examine the differentially expressed levels and redox-regulation of plasma proteins associated with type 1 diabetes mellitus, a quantitative proteomics-based approach was performed using immunodepletion of high abundance proteins, lysine- and cysteine-labeling 2D-DIGE combining MALDI-TOF/TOF MS analysis to obtain a panel of plasma proteins found to be differentially altered between type 1 diabetes mellitus patients and healthy donors in protein abundance and thiol reactivity. Importantly, one of the identified proteins, hemopexin, was evidenced to be regulated by glucose concentration which is in turn mediated through a ROS-dependent mechanism.

2. Materials and methods

2.1. Chemicals and reagents

Generic chemicals and the albumin and IgG depletion kit were purchased from Sigma-Aldrich (St. Louis, USA), while reagents for 2D-DIGE were purchased from GE Healthcare (Uppsala, Sweden). All primary antibodies were purchased from Abcam (Cambridge, UK) and anti-mouse and anti-rabbit horseradish peroxidase conjugated secondary antibodies were purchased from GE Healthcare (Uppsala, Sweden). All chemicals and biochemicals used in this study were of analytical grade.

2.2. Cell lines and cell cultures

The cell lines ARPE-19 cells, Chang's liver cells, HeLa cells and HT29 cells were purchased from the American Type Culture Collection (Manassas, VA) and were maintained in Dulbecco's Modified Eagle's medium (DMEM) supplemented with 10% (v/v) fetal calf serum (FCS), L-glutamine (2 mM), streptomycin (100 µg/mL), and penicillin (100 IU/mL) (all from Gibco-Invitrogen Corp., UK). All cells were incubated at 37 °C and 5% CO₂.

For cell culturing at differential glucose concentrations, the cultures were exposed to D-glucose at a final concentration of 25 and 100 mM (corresponding to 2 h after meal plasma glucose level of diabetic patients and glucose level in uncontrolled diabetic patients [21], respectively) and compared with cultures exposed to 5.5 mM D-glucose as control (corresponding to fasting plasma glucose level of type 1 DM-free people) [22,23]. To exclude the possible effects of hyperosmotic stress, mannitol was used to balance the differential glucose concentrations according to a previous report [24]. After exposure for at least 3 weeks, the monolayer cultures were used for further analysis.

2.3. Plasma sample collection and immunodepletion

From Jan 2009 to Dec 2009, twenty donors in a single center (Chiayi Christian Hospital, Chiayi, Taiwan) were enrolled into the study. Those included in the study were divided into type 1 diabetes mellitus (n=15) and healthy donor groups (n=5). The criteria to assess the presence of type 1 diabetes mellitus

were based on the guidelines proposed by the World Health Organization. All type 1 diabetic patients had typical diabetic symptoms along with a single fasting plasma glucose level of >7 mM or 2 h postprandial plasma glucose level of >11.1 mM. Healthy individuals with their fasting blood glucose below 5.5 mM were selected as controls. This study was approved by the Institutional Research Board and carried out according to the Helsinki Declaration Principles. Written informed consent was collected from all participating subjects.

To improve the performance of proteomic analysis of the plasma samples, the albumin and immunoglobulin G in the collected plasma samples were depleted using an albumin and IgG removal kit (Sigma, St. Louis, USA) according to the manufacturer's instructions. The depleted plasma samples were precipitated by adding 1 volume of 100% TCA (at -20 °C) to 4 volumes of sample and incubated for 10 min at 4 °C. The precipitated protein was then recovered by centrifugation at 13,000 rpm for 10 min, and the resulting pellet was washed twice with ice-cold acetone. Air-dried pellets were resuspended in 2-DE lysis containing 4% w/v CHAPS, 7 M urea, 2 M thiourea, 10 mM Tris-HCl, pH 8.3, 1 mM EDTA for expression 2D-DIGE analysis or resuspended in 4% w/v CHAPS, 8 M urea, 10 mM Tris-HCl pH 8.3 and 1 mM EDTA for redox DIGE analysis. Protein concentrations were determined using the Coomassie Protein Assay Reagent (BioRad).

2.4. 2D-DIGE and image analysis

For expression 2D-DIGE, protein samples were labeled with N-hydroxysuccinimidyl ester-derivatives of the cyanine dyes Cy2, Cy3 and Cy5 following the protocol described previously [25,26]. Briefly, 150 μ g of protein sample was minimally labeled with 375 pmol of either Cy3 or Cy5 for comparison on the same 2-DE. To facilitate image matching and cross-gel statistical comparison, a pool of all samples was also prepared and labeled with Cy2 at a molar ratio of 2.5 pmol Cy2 per μ g of protein as an internal standard for all gels. The labeling reactions were performed in the dark on ice for 30 min and then quenched with a 20-fold molar ratio excess of free L-lysine to dye for 10 min. The differentially Cy3- and Cy5-labeled samples were then mixed with the same amount of Cy2-labeled internal standard and reduced with 65 mM dithiothreitol for 10 min. IPG buffer, pH 3–10 nonlinear (2% (v/v), GE Healthcare) was added and the final volume was adjusted to 450 μ L with 2D-lysis buffer for rehydration. Immobilized pH gradient (IPG) strips (pH 3–10NL, 24 cm) were rehydrated with the CyDye-labeled samples in the dark at room temperature overnight. Isoelectric focusing was then performed using a Multiphor II apparatus (GE Healthcare) for a total of 62.5 kWh at 20 °C. Strips were equilibrated in 6 M urea, 30% (v/v) glycerol, 1% SDS (w/v), 100 mM Tris-HCl (pH 8.8) with 65 mM dithiothreitol for 15 min and then in the same buffer containing 240 mM iodoacetamide for a further 15 min. The equilibrated IPG strips were transferred onto 24 \times 20 cm 12.5% polyacrylamide gels casted between low fluorescent glass plates. The strips were overlaid with 0.5% (w/v) low melting point agarose in running buffer containing bromophenol blue. The gels were run in an Ettan Twelve gel tank (GE Healthcare) at 4 W per gel at 10 °C until the dye front had completely run off the bottom of the gels. Afterward, gels were scanned

directly between the glass plates using an Ettan DIGE Imager (GE Healthcare). Image analysis was performed using DeCyder 2-D Differential Analysis Software v7.0 (GE Healthcare) to co-detect, normalize and quantify the protein features in the images. Features detected from non-protein sources (e.g. dust particles and dirty backgrounds) were filtered out. Spots displaying a >1.3 average-fold increase or decrease in abundance with a p-value <0.05 were selected for protein identification.

For redox DIGE analysis, protein samples were labeled with ICy3 or ICy5 (80 pmol/ μ g protein) on ice. Test samples were labeled with the ICy3 dye and mixed with an equal amount of a standard pool of both samples labeled with ICy5. The reactions were left in the dark for 1 h followed by labeling with Cy2 for a further 30 min to facilitate subsequent image matching between dye-labeled proteins and colloidal Coomassie Blue-stained proteins. The reactions were quenched with DTT (65 mM final concentration) for 10 min followed by L-lysine for a further 10 min. Volumes were adjusted to 450 μ L with buffer plus DTT and IPG buffer for rehydration. Individual pooled samples were run in duplicate against the standard pool [27].

2.5. Protein staining

Colloidal Coomassie Blue G-250 staining was used to visualize CyDye-labeled protein features in 2-DE gels. Bonded gels were fixed in 30% v/v ethanol, 2% v/v phosphoric acid overnight, washed three times (30 min each) with ddH₂O and then incubated in 34% v/v methanol, 17% w/v ammonium sulfate, 3% v/v phosphoric acid for 1 h, prior to adding 0.5 g/L Coomassie Blue G-250. The gels were then left to stain for 5–7 days. No destaining step was required. The stained gels were then imaged on an ImageScanner III densitometer (GE Healthcare).

2.6. In-gel digestion

Excised gel pieces were washed three times in 50% acetonitrile, dried in a SpeedVac for 20 min, reduced with 10 mM dithiothreitol in 5 mM ammonium bicarbonate pH 8.0 for 45 min at 50 °C and then alkylated with 50 mM iodoacetamide in 5 mM ammonium bicarbonate for 1 h at room temperature in the dark. The gel pieces were then washed three times in 50% acetonitrile and vacuum-dried before re-swelling with 50 ng of modified trypsin (Promega) in 5 mM ammonium bicarbonate. The pieces were then overlaid with 10 μ L of 5 mM ammonium bicarbonate and trypsinized for 16 h at 37 °C. Supernatants were collected, peptides were further extracted twice with 5% trifluoroacetic acid in 50% acetonitrile and the supernatants were pooled. Peptide extracts were vacuum-dried, resuspended in 5 μ L ddH₂O, and stored at -20 °C prior to MS analysis.

2.7. Protein identification by MALDI-TOF MS

MALDI-TOF MS with peptide mass fingerprinting (PMF) was employed for protein identification. Briefly, 0.5 μ L of trypsin digested sample was mixed with 0.5 μ L of a matrix solution containing α -cyano-4-hydroxycinnamic acid at a concentration of 1 mg/mL in 50% acetonitrile (v/v)/0.1% trifluoroacetic acid (v/v) and spotted onto an anchorchip target plate (Bruker Daltonics) and dried. The peptide mass fingerprints were

acquired using an Autoflex III mass spectrometer (Bruker Daltonics) in reflector mode. The algorithm used for spectrum annotation was SNAP (Sophisticated Numerical Annotation Procedure). This process used the following detailed metrics: peak detection algorithm: SNAP; signal-to-noise threshold: 25; relative intensity threshold: 0%; minimum intensity threshold: 0; maximal number of peaks: 50; quality factor threshold: 1000; SNAP average composition: averaging; baseline subtraction: median; flatness: 0.8; median level: 0.5. The spectrometer was also calibrated with a peptide calibration standard (Bruker Daltonics) and internal calibration was performed using trypsin autolysis peaks at m/z 842.51 and m/z 2211.10.

Peaks in the mass range of m/z 800–3000 were used to generate a peptide mass fingerprint that was searched against the Swiss-Prot/TrEMBL database (release on 05-Oct-10) with 521,016 entries using Mascot software v2.3.02 (Matrix Science, London, UK). The following parameters were used: *Homo sapiens*; tryptic digest with a maximum of 1 missed cleavage; carbamidomethylation of cysteine, partial protein N-terminal acetylation, partial methionine oxidation, partial modification of glutamine to pyroglutamate, ICy3 (C34 H44 N3 O) and ICy5 (C34 H42 N3 O) and a mass tolerance of 50 ppm. Identifications were accepted based on significant MASCOT scores ($P < 0.05$), at least 4 peptides per protein, spectral annotation and

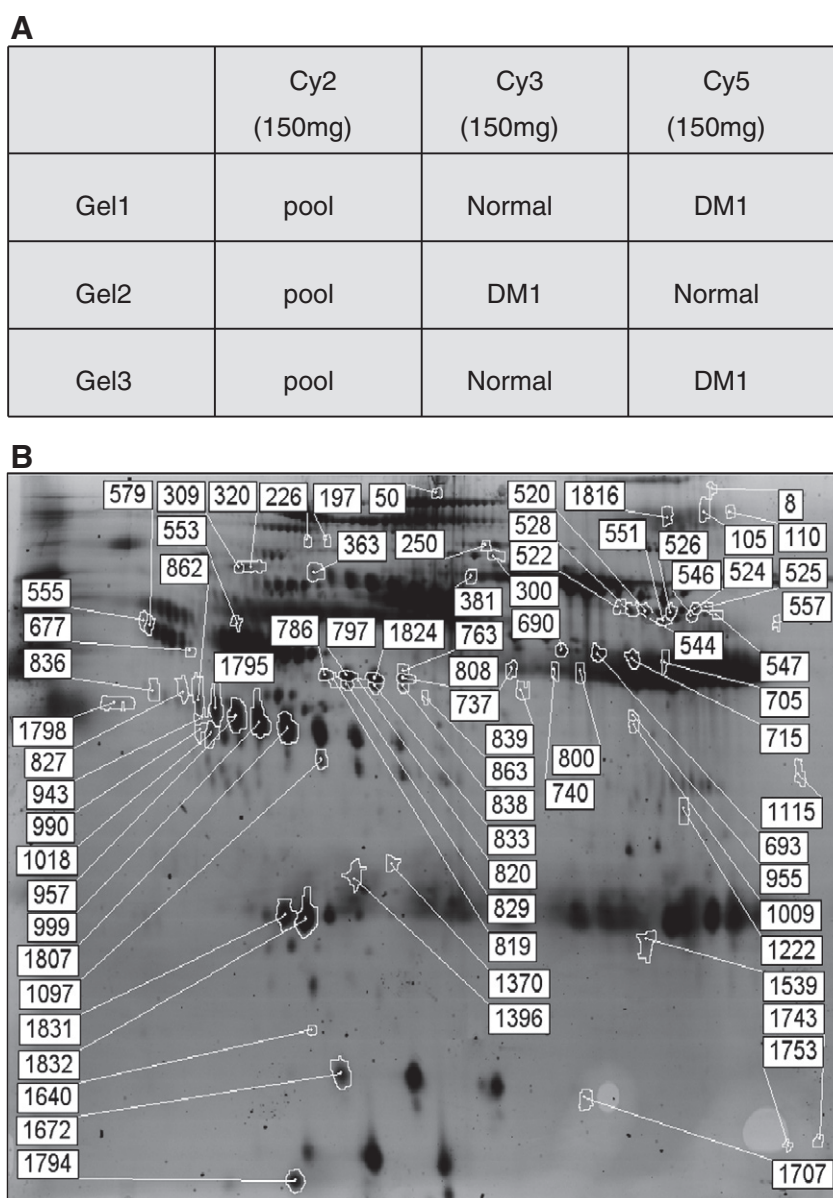


Fig. 1 – 2D-DIGE comparative analysis of plasma from type 1 diabetes mellitus cases and healthy controls. (A) Pooled plasma sample arrangement for a triplicate 2D-DIGE experiment. (B) Plasma samples (150 μ g each) were labeled with Cy-dyes and separated using 24 cm, pH 3–10 non-linear IPG strips. The differentially expressed identified protein features in 2D-DIGE are annotated with spot numbers.

observed versus expected molecular weight and pI on 2-DE gels. MALDI-TOF/TOF analysis was performed on the same instrument using the LIFT mode. MS/MS ion searches were performed using Mascot with the same search parameters as above and using an MS/MS tolerance of ± 0.2 Da.

2.8. Immunoblotting

Plasma samples or cell lysates were quantified using Coomassie Protein Assay Reagent (BioRad). 30 μ g of protein sample was diluted in Laemmli sample buffer (final concentrations: 50 mM Tris pH 6.8, 10% (v/v) glycerol, 2% SDS (w/v), 0.01% (w/v) bromophenol blue) and separated by 1D-SDS-PAGE following standard procedures. After electroblotting proteins onto 0.45 μ m Immobilon P membranes (Millipore), the membranes were blocked with 5% w/v skimmed milk in TBS-T (50 mM Tris pH 8.0, 150 mM NaCl and 0.1% Tween-20 (v/v)) for 1 h. Membranes were then incubated in primary antibody solution in TBS-T for 2 h. Membranes were washed in TBS-T (3 \times 10 min) and then probed with the appropriate horseradish peroxidase-coupled secondary antibody (GE Healthcare). After further washing with TBS-T, immunoprobed proteins were visualized using an enhanced chemiluminescence method (Visual Protein Co.).

2.9. MTT cell viability assay

Cells growing exponentially were trypsinized, counted using a hemocytometer and 10,000 cells/well were seeded into 96-well plates. The culture was then incubated for 24 h before pre-treatment with the indicated concentrations of berberine for 24 h or left untreated. After removal of the medium, 50 μ L of MTT working solution (1 mg/mL) (Sigma) was added to the cells in each well, followed by a further incubation at 37 $^{\circ}$ C for 4 h. The supernatant was carefully removed. 100 μ L of DMSO was added to each well and the plates shaken for 20 min. The absorbance of samples was then measured at 540 nm in a multi-well plate reader. Values were normalized against the untreated samples and were averaged from 4 independent measurements.

2.10. Assay for endogenous reactive oxygen species (ROS) using DCFH-DA

Cells (10,000 cells/well) were incubated with the indicated concentrations of glucose for 20 min. After two washes with PBS, cells were treated with 10 μ M of 2, 7-dichlorofluorescein diacetate (DCFH-DA; Molecular Probes) at 37 $^{\circ}$ C for 20 min, and subsequently washed with PBS. Fluorescence was recorded by Ettan DIGE Imager (GE Healthcare) at an excitation wavelength at 485 nm and emission wavelength at 530 nm.

2.11. Assay for the effect of reduced glutathione on glucose-induced hemopexin expression

To examine the effect of reduced glutathione (GSH) on glucose-induced hemopexin expression, cells growing in 25 mM glucose were treated with reduced GSH (10 and 20 mM) or vehicle (serum free medium) for 2 h. The cells were lysed to monitor the hemopexin levels with immunoblotting described previously.

2.12. Enzyme-linked immunosorbent assay (ELISA) analysis

EIA polystyrene microtiter plates were coated with 50 μ g of protein sample and incubated at 37 $^{\circ}$ C for 2 h. The plate was washed three times with phosphate buffered saline with Tween-20 (PBS-T) and three times with PBS. Plates were then blocked with 100 μ L of 5% skimmed milk in PBS at 37 $^{\circ}$ C for 2 h and then washed three times with PBST. Hemopexin and haptoglobin antibodies (Abcam) solution were added and incubated at 37 $^{\circ}$ C for 2 h. After washing with PBST and PBS for 10 times in total, 100 μ L of peroxidase-conjugated secondary antibody in PBS was added for incubation at 37 $^{\circ}$ C for 2 h. Following 10 washes, 100 μ L of 3,3',5,5'-tetramethyl benzidine (Pierce) was added. After incubation at room temperature for 30 min, 100 μ L of 1 M H₂SO₄ was added to stop the reaction and the absorbance at 450 nm measured using a Stat Fax 2100 microtiter plate reader (Awareness Technology Inc., FL, USA).

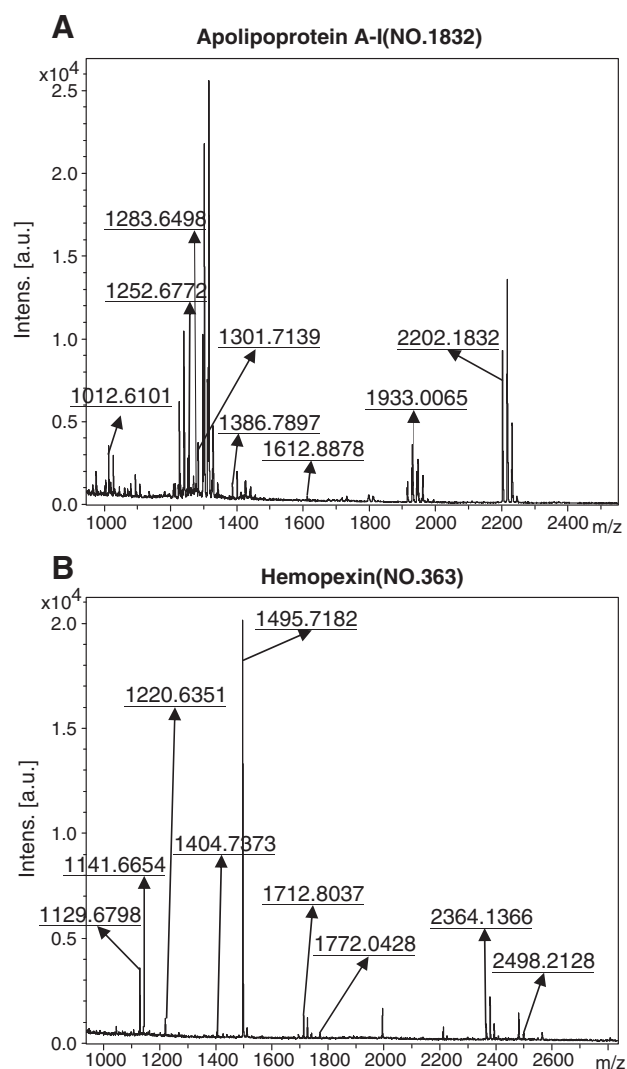


Fig. 2 – Peptide mass fingerprinting of identified proteins apolipoprotein A-I and hemopexin.

Table 1 – List of differentially expressed plasma proteins between type 1 diabetic patients (n=15) and healthy individuals (n=5) as identified by MALDI-TOF peptide mass fingerprinting following 2D-DIGE analysis.

Protein name	pI	MW	Peptide matches	Coverage (%)	Score	MS p-value	MS/MS p-value	DM1/normal ^a	t-test	Matched peptide sequences ^b	Subcellular location	Functional Ontology
Actin-binding protein anillin	8.38	125490	6/9	5	58/56	0.031	N.A.	-1.39	0.047	R.LLTSITTK.S; R.FGERCQEHSK.E	Nucleus	Nucleus
Apolipoprotein A-I ^c	5.56	30759	8/26	31	82/56	0.00012	0.0032	1.48	0.011	K.LREQLGVPVTEFWDNLEK.E; K.AKPALEDLR.Q; (R.THLAPYSDEL.R.Q)	Secreted	Cholesterol transport
Carnitine O-palmitoyltransferase I, liver isoform	8.85	88995	6/12	10	60/56	0.019	N.A.	-1.76	0.032	R.LAMTGSIDRHLFCLYVVS.K.Y; K.VLLSYHGWMFTEHGKMSR.A	Mitochondria	Lipid metabolism
Cytoplasmic dynein 1 light intermediate chain 1	6.01	56829	5/12	13	58/56	0.03	N.A.	-1.88	0.018	K.IPAVVVEKDAVFIPAGWDNDK.K; K.QMEQKLIR.D	Cytoplasm	Protein trafficking
DCC-interacting protein 13-beta	4.87	74959	6/12	18	70/56	0.002	N.A.	1.48	0.023	K.QLLAYEK.Q; R.RTNPFGETEDESFPAAEDSLLQQMFIVR.F	Nucleus	Cell proliferation
DNA mismatch repair protein Mlh1	5.51	85175	8/13	8	84/56	8.30E-05	N.A.	-3.38	0.00072	K.CAYRASYSYDQK.L; K.LLGSNSSR.M	Nucleus	DNA repair
Exocyst complex component 3	5.8	87303	5/7	9	59/60	0.028	N.A.	1.52	0.0059	K.TKVLVLCQQMNSFLSR.Y; R.DDHIGALLAVR.G	Cytoplasm	Protein transport
FGFR1 oncogene partner 2	5.69	29522	5/9	13	58/56	0.029	N.A.	-1.66	0.0078	R.QIRELQENK.E; R.ELQENKELR.T	Cytoplasm	Signal transduction
Fibrinogen beta chain ^d	8.54	56577	6/18	14	71/56	0.0016	N.A.	-2.63	0.001	K.GSWYSMR.K; R.SILENLR.S	Secreted	Coagulation
Fibrinogen beta chain ^d	8.54	56577	6/9	11	60/56	0.021	N.A.	-2.63	0.0014	K.IRPFPPQQ.-; K.EDGGWVWYR.C	Secreted	Coagulation
Fibrinogen gamma chain ^{c,d}	5.37	52106	6/12	13	70/56	0.0019	0.00086	-2.13	0.038	K.IHLISTQSAIPYALR.V; K.IIPFNR.L; (K.IHLISTQSAIPYALR.V)	Secreted	Coagulation
Fibrinogen gamma chain ^d	5.37	52106	10/19	23	106/56	5.10E-07	N.A.	-2.38	0.037	R.LTIGEGQQHHLGGAK.Q; K.QSGLYFIKPLK.A	Secreted	Coagulation
Fibrinogen gamma chain ^d	5.37	52106	6/9	14	81/56	0.00017	N.A.	-2.82	0.0034	K.IHLISTQSAIPYALR.V; K.YEASILTHDSSIR.Y	Secreted	Coagulation
Haptoglobin ^c	6.13	45861	10/30	26	103/56	1.00E-06	3.50E-09	1.39	0.047	K.VTSIQDWWVQK.T; K.DIAPTLTYVVGK.K; (K.VVLHPNYSQVDIGLIK.L)	Secreted	Inflammatory response
Hemopexin ^c	6.55	52385	9/21	27	100/56	2.00E-06	0.00011	2.3	0.004	K.EVGTPHGILDSVDAAFICPGSSR.L; K.LLQDEFFGPIPLDAAVECHR.G; (K.NFPSPVDAAFR.Q)	Secreted	Heme transport
Ig mu chain C region	6.35	49960	5/6	11	62/56	0.012	N.A.	1.34	0.0093	K.LICQATGFSPR.Q; R.QIQVSWLR.E	Secreted	Inflammatory response
Oral-facial-digital syndrome 1	5.82	117055	6/8	8	60/56	0.018	N.A.	2.03	0.047	R.LSSTPLPK.A; R.NQLIHELMHPVLSGELQPR.S	Cytoplasm	Cell signaling
Parafibromin	60653	9.63	6/16	15	62/56	0.014	N.A.	1.34	0.048	K.GKEETEGFK.I; -.MADVLSVLR.Q	Nucleus	Cell cycle regulation
Polypeptide N-acetylgalactosaminyltransferase 2	8.63	65433	6/8	11	60/56	0.02	N.A.	-3.76	0.008	K.YDMMMDVWGGENLEISFR.V; R.VGHVFRK.Q	Golgi	Protein glycosylation
Prenyltransferase alpha subunit repeat containing protein 1	6.5	46718	5/11	8	58/56	0.032	N.A.	1.39	0.035	R.IWVLQHLAK.L; K.WLVTLISQ.-	Cytoplasm	Protein modification

Probable rRNA-processing protein EBP2	10.1	34887	5/8	18	59/56	0.028	N.A.	-3.59	0.00056	R.EMSFYR.Q; R.ELQDAFSR.G	Nucleus	Gene regulation
Prothrombin	5.64	71475	8/20	18	81/56	0.00015	N.A.	-2.36	0.018	K.YGFYTHVFR.L; R.TATSEYQTFNPR.T	Secreted	Coagulation
Radixin	6.03	68635	9/16	12	74/56	0.00081	N.A.	1.5	0.016	R.IDEFEAM.-; K.EQWEER.I	Cell membrane	Cytoskeleton regulation
Retinoic acid receptor RXR-gamma	7.55	51580	6/10	8	60/56	0.018	N.A.	-3.13	0.00023	K.SELGCLR.A; K.CLVMGMK.R	Nucleus	Gene regulation
Rho GTPase-activating protein 25	5.83	72955	6/14	13	58/56	0.035	N.A.	-1.34	0.0061	K.MSVDNLATVIGVNLIRSK.V; K.VEDPAVIMR.G	Cytoplasm	Signal transduction
RNA-binding protein 34	10.11	48649	6/12	12	72/56	0.0011	N.A.	1.35	0.013	K.LADRESALASADLEEEIHQK.Q; K.QQNSNPRK.N	Nucleus	Gene regulation
Semenogelin-2/SGII	9.08	65519	5/10	16	61/56	0.016	N.A.	1.59	0.022	K.STQKDVSSISFQIEK.L;	Secreted	Reproduction
Serine/threonine-protein phosphatase 4 regulatory subunit 3A	4.83	95935	6/10	6	58/56	0.031	N.A.	-2.42	0.003	K.AGCDEIWEK.I; R.RVLVLMASK.H	Cytoplasm	Signal transduction
Serum amyloid P-component ^c	6.1	25485	5/15	24	74/56	0.00076	0.00051	-1.31	0.019	R.AYSLFSYNTQGR.D; R.QGYFVEAQPK.I;	Secreted	Transport
Shootin-1	5.27	72109	5/7	9	56/56	0.046	N.A.	-1.83	0.01	R.ISMLYMAK.L; K.ATQPETTEVTDLK.R	Cell projection	Cell polarization
Sorting nexin-29	6.14	48308	5/14	8	60/56	0.022	N.A.	-3.22	0.00061	R.QATVAMMNRK.D; R.QGMKVQALAR.E	Cytoplasm	Protein trafficking
Succinyl-CoA:3-ketoacid-coenzyme A transferase 1	7.14	56578	6/11	15	74/56	0.00078	N.A.	-3.08	9.90E-05	R.HTKFYTDPVEAVK.D; K.LMPMQQIAN.-	Mitochondria	Metabolism
Synaptojanin-1	2E	7.13	7/10	7	66/56	0.0056	N.A.	1.85	0.012	K.SPDWIKNLEEEMSLEK.I; K.ISNPKGWVTFEEEDFGVK.G	Cytoplasm	Endocytosis
TNFAIP3-interacting protein 1	6.23	72105	9/22	13	83/56	9.30E-05	N.A.	1.44	0.0066	M.EGRGPYR.I; K.QQYEQK.I	Cytoplasm	Signal transduction
Uncharacterized protein KIAA0082	6.64	96172	6/9	9	57/56	0.043	N.A.	-1.43	0.023	R.HFVPMGLYIVR.T; K.IHAFVQDTTLSEPRQAEIR.K	Nucleus	Translation regulation
Vasohibin-2	10.02	40595	6/10	18	62/56	0.013	N.A.	-2.2	0.0014	R.TLSDLIFDFEDSYKK.Y; K.MRPLSGLMETAK.E	Cytoplasm	Angiogenesis inhibitor
Zinc finger BED domain-containing	5.79	78904	5/8	10	58/56	0.032	N.A.	-3.11	6.20E-05	M.ENKSLESSQTDLK.L; K.LVEYFQQSAVAMYLYEK.Q	Nucleus	Signal transduction
Zinc finger protein SNAI3	9.45	33422	5/17	13	60/56	0.022	N.A.	1.94	0.0072	R.VPNYRR.L; M.PRSFLVK.T	Nucleus	Signal transduction
Zinc-alpha-2-glycoprotein	5.57	34079	6/21	21	61/56	0.015	N.A.	1.62	0.0066	K.EIPAVWVPDPAAQITK.Q; K.WEAEFVYVQR.A	Secreted	Lipid degradation

^a Average fold-differences of replicate samples run on different gels from DeCyder analysis show abundance ratios for type 1 diabetic plasma versus healthy donor's plasma. Proteins displaying an average fold-difference of 1.3-fold up or downregulation where $p < 0.05$ and spots matched in all images are listed in the Table. Functions were ascribed from the Swiss-Prot databases and literature searches.

^b In MS analysis, we listed top 2 score peptide sequences in the matched peptide column. In MS/MS analysis, we listed the MS/MS-sequenced peptide with bracket in the matched peptide column.

^c Proteins identified by MALDI-TOF/TOF.

^d Proteins appearing more than once were identified as isoforms with different % coverage of analyzed peptides, matched peptide numbers, MOWSE scores, p-values of MS and MS/MS search, average fold-differences, t-test values and matched peptide sequences for each identified protein.

2.13. Validation of thiol reactivity changes by immunoprecipitation coupled to fluorescent immunoblotting

Albumin and IgG-depleted plasma samples (500 µg total protein) from 15 type 1 DM patients and 5 healthy donors) were labeled with ICy3 or ICy5 dyes as described above and then diluted 20-fold with buffer containing 50 mM HEPES pH 7.4, 150 mM NaCl, 1% NP40, 1 mM EDTA, 2 mM sodium orthovanadate, 100 µg/mL AEBSF, 17 µg/mL aprotinin, 1 µg/mL leupeptin, 1 µg/mL pepstatin, 5 µM fenvalerate, 5 µM BpVphen and 1 µM okadaic acid. This was then incubated with 5 µg primary antibody and 40 µL of a 50% slurry of protein A-Sepharose for 16 h at 4 °C. Immune complexes were then washed three times in lysis buffer and boiled in Laemmli sample buffer prior to resolving by SDS-PAGE. Gels were scanned directly between low-fluorescence glass plates using an Ettan DIGE Imager (GE Healthcare).

3. Results

3.1. 2D-DIGE and mass spectrometry analysis of the immunodepleted plasma proteome

In order to study the alteration of plasma proteins in type 1 diabetic patients, a 2D-DIGE-based comparative proteomic analysis was performed on samples from patients with type 1 diabetes versus healthy donors using albumin and IgG depletion to enhance the visualization of lower abundance proteins. Pooled samples containing plasma from type 1 diabetes mellitus patients (n=15) and healthy donors (n=5) were minimally labeled with Cy3 and Cy5 dyes and run in triplicate against a Cy2-labeled internal standard (pool of all samples) (Fig. 1A). Image analysis indicated 89 protein features showing a >1.3-fold change in expression level ($P < 0.05$) between the two groups (Fig. 1B). MALDI-TOF/TOF MS analysis identified 39 proteins from these excised features (Fig. 2, Table 1 and Supplementary Figure). Most of the identified proteins are secreted proteins (33%), but nuclear

(26%) and cytoplasmic proteins (15%) were also represented. In terms of known function, the majority of proteins are involved in coagulation (15%) and signal transduction (15%) (Fig. 3). Representative examples of proteins showing altered spot intensities are displayed in Fig. 4.

3.2. Validation by immunoblotting and ELISA

To verify the abundance changes in hemopexin and haptoglobin found in the 2D-DIGE/MS analysis, their levels were investigated by immunoblotting and ELISA. As is shown in Fig. 5A, 52 kDa and 46 kDa bands corresponding to hemopexin and haptoglobin respectively, were increased in the plasma of patients with type 1 diabetes mellitus. Additionally, ELISAs were performed on the individual samples to measure plasma hemopexin and haptoglobin levels, revealing an increase in the levels of both in the type 1 diabetes mellitus samples compared to the healthy controls (Fig. 5B).

3.3. Glucose induces hemopexin expression through an ROS-dependent mechanism

Hemopexin is an acute-phase serum glycoprotein, expressed mainly by the liver and released into the circulation where it serves as a plasma heme scavenger and transports toxic plasma heme to the liver. Other reported sites for hemopexin synthesis are the skeletal muscle, retina, nervous system and kidney [28]. In order to examine the effect of glucose on hemopexin expression, cell lines including a retinal cell line (ARPE-19), a normal liver cell line (Chang's liver cells), a cervical cancer cell line (HeLa) and a colon cancer cell line (HT29) were cultured in 5.5 mM, 25 mM and 100 mM glucose corresponding to normal, 2 h after meal plasma glucose level of type 1 DM patients and glucose level in in vitro cell culture only, respectively. For at least 3 week incubation, there was no significant change in cell viability in any of the culture models as monitored by MTT assay (Fig. 6A). Subsequently, cells were maintained in 5.5 mM, 25 mM and 100 mM glucose and the effect on hemopexin expression monitored by immunoblotting.

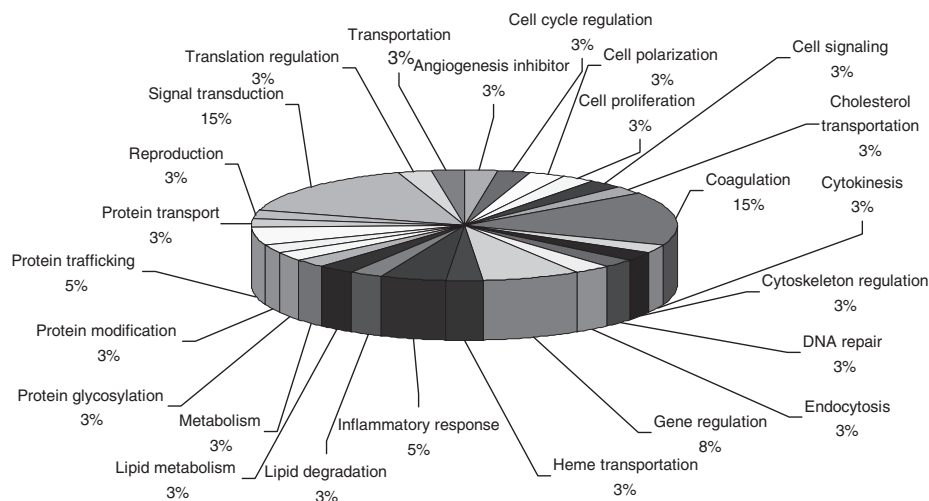


Fig. 3 – Distribution of biological functions for identified differentially expressed proteins. Functions were taken from the SwissProt database.

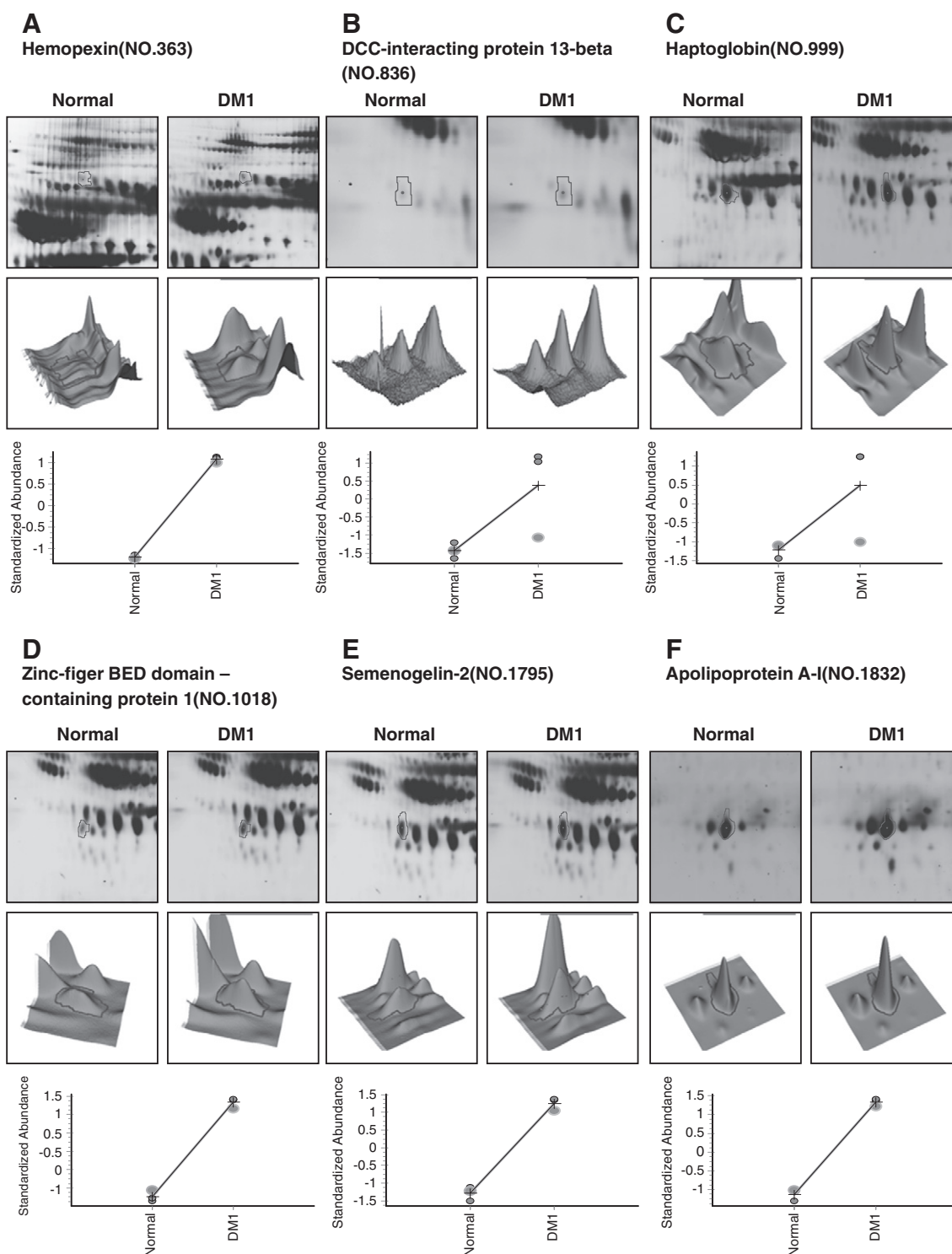


Fig. 4 – Representative images of the identified spots ((A) hemopexin; (B) DCC-interacting protein 13-beta; (C) haptoglobin ; (D) zinc finger BED domain containing protein 1; (E) semenogelin-2; (F) apolipoprotein A-I) displaying type 1 diabetes mellitus-dependent protein expression changes. The levels of these proteins are visualized as 2-DE images (top panels), three-dimensional spot images (middle panels) and protein expression maps (bottom panels). All of statistic comparisons used in this study were performed with two group student t-test.

The results demonstrated that glucose treatment increased hemopexin expression in all four cell models (Fig. 6B). High glucose has been reported to induce ROS generation [29]. We

thus hypothesized that glucose-induced hemopexin expression might be modulated by ROS. For this, a DCFH assay was used to monitor ROS production in Chang's liver cells grown at different

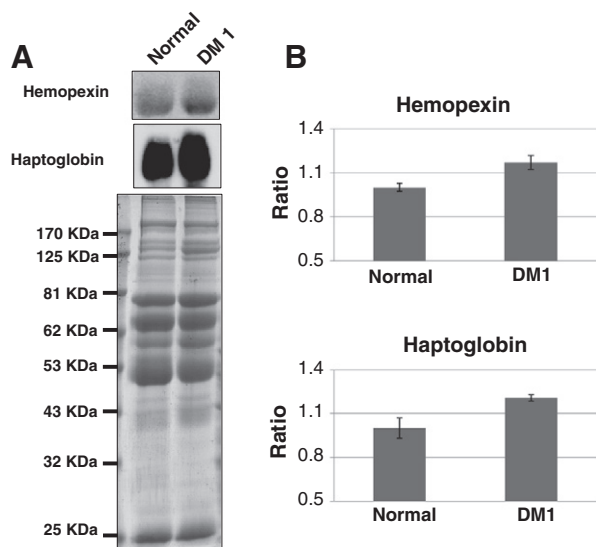


Fig. 5 – Immunoblotting and ELISA analysis of hemopexin and haptoglobin in type 1 diabetes mellitus plasma and healthy control plasma. (A) 20 μ g of the albumin and IgG-depleted plasma was loaded and resolved by SDS-PAGE followed by either immunoblotting with haptoglobin and hemopexin antibodies or staining with colloidal Coomassie Blue G-250 as a loading control. (B) 50 μ g of pooled plasma samples was coated onto each well of a 96-well plate for ELISA analysis of haptoglobin and hemopexin levels in plasma, and absorbance was measured at 450 nm using a Stat Fax 2100 microtiter plate reader. All of statistic comparisons used in this study were performed with two group Student's t-test.

glucose concentrations. The results showed that high concentration of glucose leads to increased ROS production in Chang's liver cells (Fig. 7A). Further experiments indicated that pretreatment of cells with the permeable anti-oxidant, reduced GSH, significantly reduced glucose-induced ROS production (Fig. 7B) and resulted in down-regulation of hemopexin expression (Fig. 7C).

3.4. Redox 2D-DIGE analysis of differential cysteine-modification in type 1 diabetes mellitus plasma

Type 1 diabetes mellitus is associated with high blood glucose which in turn may induce ROS generation to damage or deregulate cellular proteins through oxidative modification of their cysteinyl thiol groups [30]. Accordingly, we applied a recently developed redox 2D-DIGE methodology utilizing iodoacetylated ICy dyes [31] to assess possible high plasma glucose-induced changes in plasma protein thiol reactivity. Pooled plasma from type 1 diabetes mellitus or healthy donors were labeled with ICy3 in duplicate. Individual ICy3-labeled samples were then run on 2D gels against an equal load of ICy5-labeled standard pool comprising an equal mixture of both sample types (Fig. 8A). After being analyzed with DeCyder software, 119 protein features displayed significant differences with cut-off at >1.3 average-fold increase or decrease in labeling (Fig. 8B). CCB post-staining and matching with fluorescence images allowed confident picking and identification of 41 protein species (26

unique gene products) by MALDI-TOF peptide mass fingerprinting or MALDI-TOF/TOF peptide sequence analysis (Table 2, Fig. 8C and Supplementary Figure). All of the identified proteins contain at least one cysteine residue, and since the ICy dyes target reduced cysteinyl thiols, these results suggest the altered oxidative status of some of these thiol groups in type 1 diabetes mellitus plasma. Indeed, two putative sites of thiol modification on two proteins were inferred, based on the added mass of the ICy dyes in MALDI-TOF MS spectra (Table 2). The differentially labeled proteins were mostly secreted proteins and fell into several functional groups including coagulation and transport (Fig. 9 and Table 2). Interestingly, hemopexin displayed a decrease in ICy dye labeling in type 1 diabetes mellitus plasma rather than in control donor's plasma. Thus, their free thiol groups must be oxidized in response to type 1 diabetes mellitus to block ICy labeling, implying possible oxidative damage and deregulation of this protein.

3.5. Verification of redox-induced changes in hemopexin

Immunoprecipitation combined with ICy dye fluorescence-detection was performed to compare the free thiol group content of hemopexin from type 1 diabetes mellitus versus healthy donor plasma and confirmed the decrease in free thiol content of this protein (Fig. 10A). After normalizing for the altered expression level of hemopexin in type 1 diabetic patients versus healthy donors (Fig. 5A), the adjusted thiol reactivity alteration of hemopexin between type 1 diabetes mellitus and healthy donors was approximately -3.7-fold (Fig. 10B).

4. Discussion

Proteomic analyses of human diseases usually adopt a comparative method that is defined by the differential expression of the proteins under different disease states. Our 2D-DIGE/redox 2D-DIGE combined with MALDI-TOF/TOF analysis revealed 39 and 41 protein forms displaying altered expression and thiol reactivity, respectively (Tables 1 and 2). A majority of altered proteins belong to three major functional groups: coagulation, signal transduction and transportation, in which coagulation-associated plasma proteins are not only obviously down-regulated, but significantly oxidized in type 1 diabetic plasma (Tables 1 and 2). These changes may be linked with the finding that patients with type 1 diabetes exhibit a defect in coagulation derived from decreased plasma fibrinolytic potential [32]. Notably, our approach is the first report demonstrating the deregulation of coagulant ability in type 1 diabetes mellitus caused by oxidative modifications of coagulation-related plasma factors in our knowledge.

Numerous plasma transport proteins were either regulated in expression level (apolipoprotein A-I, hemopexin and serum amyloid P-component) or redox modified (apolipoprotein A-I, apolipoprotein E, hemopexin, serotransferrin, serum albumin and transthyretin) correlating with the fact that type 1 diabetic patients have symptoms such as impaired cholesterol, heme iron, lipoprotein and thyroxine transport. For example, apolipoprotein A-I is a constituent of high density lipoprotein which plays a role in cholesterol transport from the blood into the liver

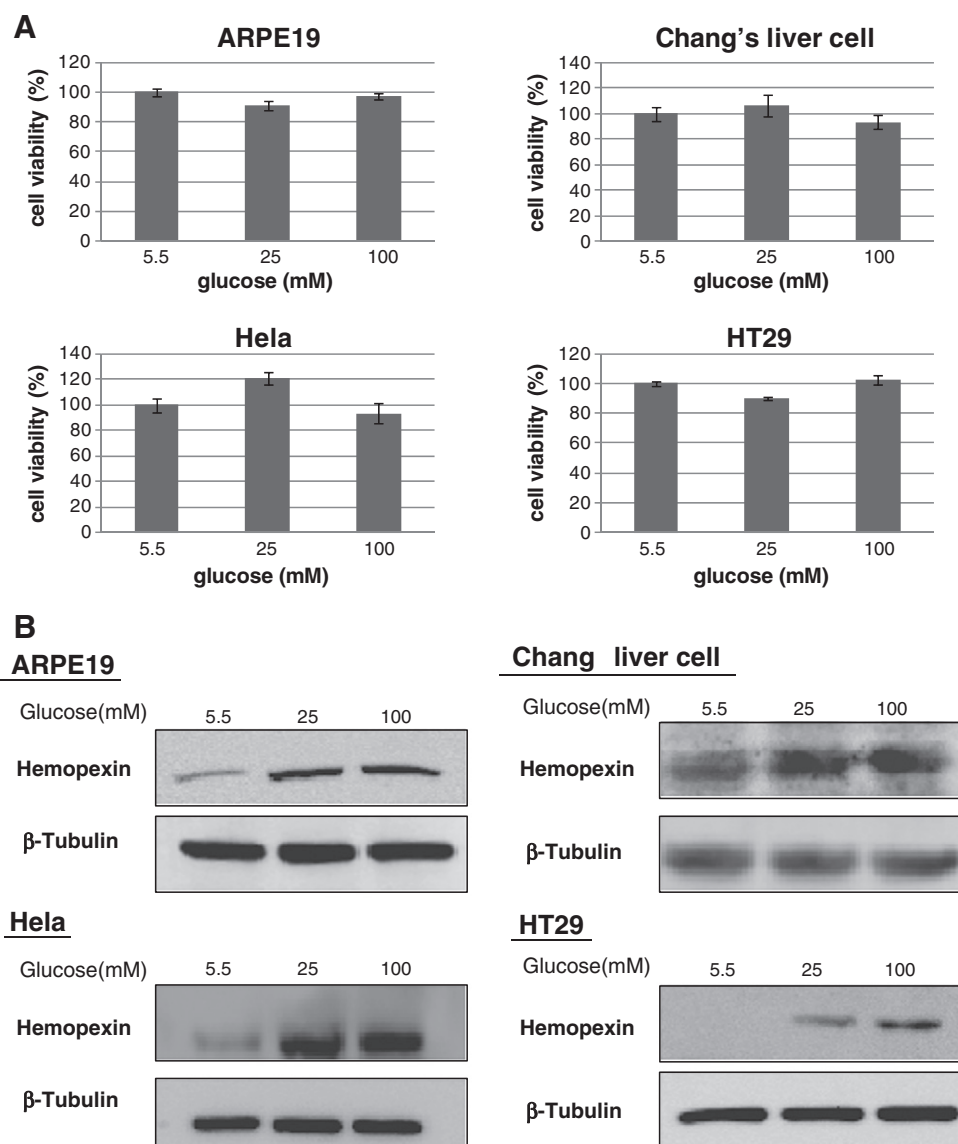


Fig. 6 – Effect of glucose concentration on cell viability and hemopexin expression in cultured cells. (A) MTT-based viability assays were performed on ARPE-19, Chang's liver, HeLa and HT29 cell cultures following 3 weeks at different glucose concentrations (5.5 mM, 25 mM and 100 mM glucose). Values were normalized against untreated samples and are the average of 4 independent measurements \pm the standard deviation. **(B)** Hemopexin expression was monitored by immunoblotting in ARPE-19, Chang's liver, HeLa and HT29 cells following treatment with different concentrations of glucose for 24 h. All of statistic comparisons used in this study were performed with two group Student's t-test.

[33]. In this study, we demonstrated that apolipoprotein A-I was up-regulated in expression level and was oxidized in type 1 diabetes mellitus plasma. This observation supports previous reports showing the relationship between apolipoprotein A-I and type 1 diabetes mellitus [34,35].

Diabetes mellitus is associated with angiopathy which leads to increase risk of peripheral ischemia and tissue damage. Development of collateral vessels of large arteries is one mechanism that minimizes the degree of ischemia injury [36]. Clinical investigations have demonstrated lower capillary density and vessel formation in ischemic cardiovascular diseases of diabetics versus non-diabetics [37,38]. In addition, recent study indicated the expression of angiogenic factors such as VEGF, angiopoietin-1 were significantly reduced in

diabetes mellitus, whereas antiangiogenic factors such as angiostatin were significantly increased in diabetes mellitus [39]. These studies indicated abnormal regulation of angiogenesis and associated signal transduction are the leading causes of diabetes-induced angiopathy. In this study, fibroblast growth factor receptor 1 (FGFR1), a receptor tyrosine kinase, was shown to be down-regulated in the plasma of type 1 diabetic patients. FGFR1 is a receptor of the fibroblast growth factors and has been implicated in proliferation and cell differentiation in many organs including the developing pancreas in mice. Mice with attenuated FGFR1 signaling exhibit a decreased number of beta-cells and develop diabetes via disrupt glucose sensing, insulin processing and glucose homeostasis [40]. Thus, the down-regulation of the FGFR1 in this study

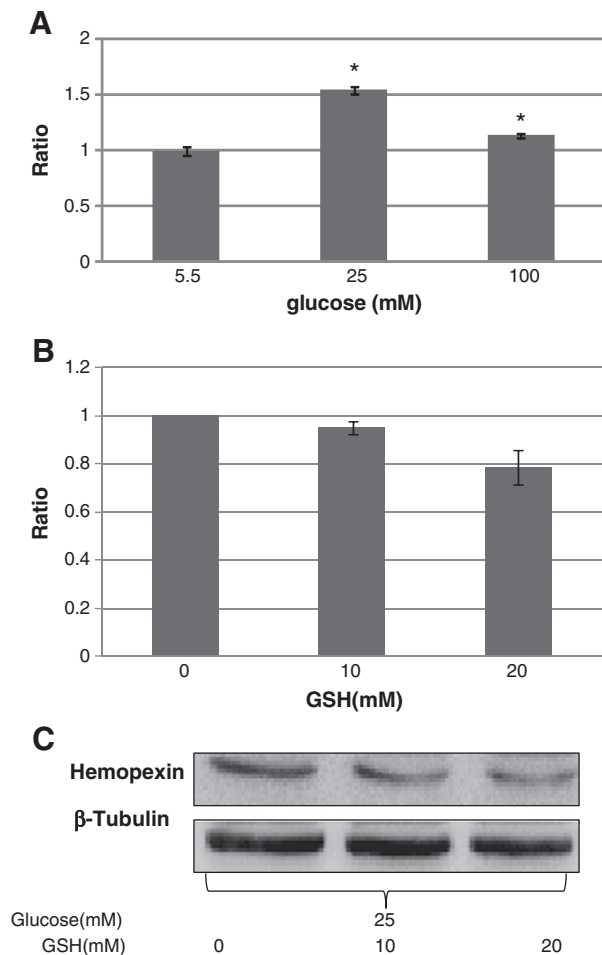


Fig. 7 – Effect of glucose concentration on ROS production and hemopexin expression in Chang's liver cells. (A) DCFH-based intracellular ROS production assays were performed where 100,000 Chang's liver cells were cultured in medium containing 5.5 mM, 25 mM and 100 mM glucose for 20 min. (B) DCFH-based intracellular ROS production assays were performed where 100,000 Chang's liver cells were plated into 24-well plates in medium containing 25 mM glucose. After 24 h, cells were pretreated with the indicated concentrations of reduced GSH or vehicle (PBS) for 2 h followed by addition of 10 μ M DCFH-DA for 20 min and the fluorescence was recorded at excitation and emission wavelengths of 485 nm and 530 nm, respectively. (C) Hemopexin expression in Chang's liver cells cultured in 25 mM glucose with pretreatment with the indicated concentrations of GSH, as monitored by immunoblotting. All of statistic comparisons used in this study were performed with two group Student's t-test.

is agreed with these previous reports and might be evaluated as a signature of type 1 diabetes mellitus in serum. Interestingly, our proteomic analysis also identified vasohibin-2 which plays roles in promoting angiogenesis [41]. The down-regulation of vasohibin-2 in type 1 diabetic plasma suggests an inhibitory effect on angiogenesis in type 1 diabetes mellitus.

Hemopexin, an acute-phase plasma glycoprotein, is produced mainly by the liver and released into plasma, in which

hemopexin binds free heme with high affinity as a heme scavenger. Heme is potentially highly toxic due to its ability to intercalate into lipid bilayers and to produce free radicals such as hydroxyl radicals. The hemopexin-heme complex can be transported to the liver, where it is catabolyzed to bile canaliculi or re-used for the synthesis of hemoproteins [42]. In this study, we demonstrated that hemopexin showed an up-regulation in expression by 2D-DIGE, immunoblotting and ELISA analysis in type 1 diabetic plasma, implying that the expression of hemopexin is modulated by factors in diabetic plasma. Additionally, our data also indicated that hemopexin was significantly oxidized in plasma from these patients. This seems to support previous data showing an increased oxidization of hemopexin in diabetic rats [43]. Importantly, human hemopexin contains 13 cysteine residues forming 6 disulfide bonds and a free thiol group at Cys-17. Accordingly, although we did not identify the site of oxidative modification, Cys-17 would be a likely target. Since Cys-17 is part of the signal sequence cleaved during secretion [44], we suggest that the oxidative modification of Cys-17 might modulate hemopexin secretion.

Hyperglycemia is a common feature of diabetes mellitus characterized by the binding of monosaccharides to amino groups of proteins. This reaction alters structure and function of proteins via the formation of advanced glycation end products and reactive oxygen species called glycooxidation [45]. Besides, glycated proteins are able to activate membrane receptors via glycation end products and induce an intracellular oxidative stress, a panel of protein kinases and a pro-inflammatory status [46–49]. In addition, excess glucose-induced ROS can promote the development of diabetic complications and cause tissue damage [50]. In this study, we demonstrated that hemopexin is expressed in multiple cell lines derived from different tissues. Importantly, increasing the glucose concentration in cell culture increased the expression of hemopexin and modulated the ROS levels in cells, which were partially reversed by adding reduced glutathione.

Clusterin is a disulfide-linked heterodimeric protein associated with various physiological disturbances that represent states of increased oxidative stress such as ischemia stress and diabetes [51]. Under oxidative stress, clusterin has shown to be up-regulated and plays a protective role in responding to the oxidized environment via the PI3K/Akt pathway [52]. Diabetes mellitus is a major risk factor for retinopathy and the oxidative stress-induced damage is a primary cause for the disease. Previous studies indicated that the antipermeability activity of clusterin was related to the alleviation of blood-retinal barrier breakdown. Additionally, clusterin can restore ischemia-induced tight junction protein loss in diabetic retinopathy [53,54]. In the current study, clusterin was shown to be oxidized in type 1 diabetes mellitus plasma, implying the function of clusterin might be perturbed leading to the loss of protective ability in diabetic retinopathy. Further study might examine the expression of clusterin in type 1 diabetic patients with or without retinopathy to evaluate the role of clusterin in the disease and its possibility to be a potential therapeutic target.

In conclusion, our quantitative proteomic approach has identified previously reported plasma markers of type 1 diabetes mellitus such as apolipoprotein A-I. Additionally, we have presented several putative type 1 diabetes mellitus

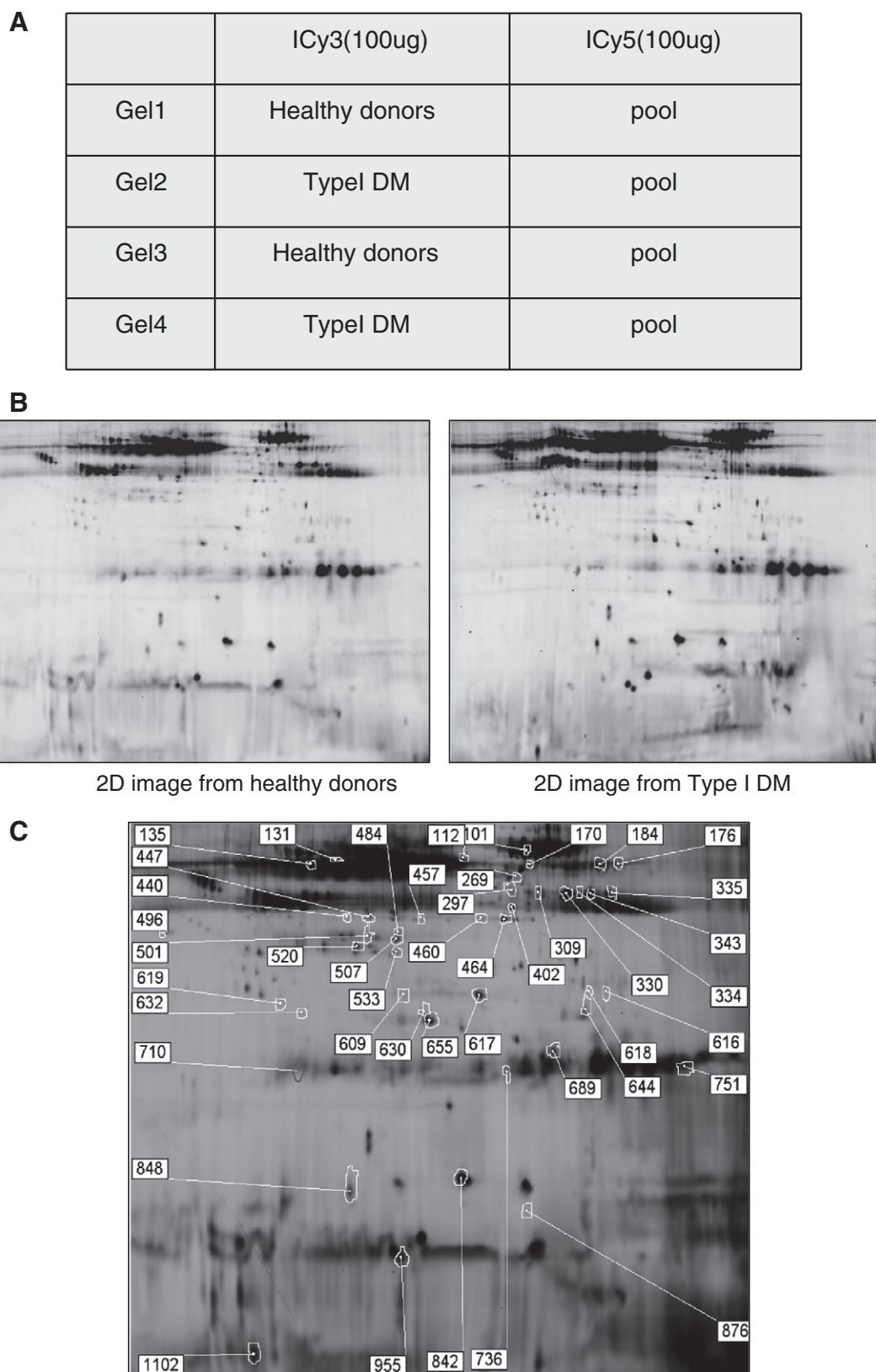


Fig. 8 – Redox 2D-DIGE analysis of type 1 diabetes mellitus-induced differential cysteine-modification in plasma. (A) Plasma samples arrangement for a duplicated redox-2D-DIGE experiment. (B) Plasma samples (50 μ g each) were labeled with ICy-dyes and separated using 24 cm, pH 3–10 non-linear IPG strips. 2D-DIGE images of the plasma samples from type 1 diabetic patients and healthy individuals at appropriate excitation and emission wavelengths were shown. (C) Differentially labeled protein features are annotated with spot numbers.

Table 2 – Differentially labeled proteins identified by cysteine labeling 2D-DIGE and MS. Plasma proteins displaying differential ICy dye labeling between type 1 diabetic patients and healthy individuals were identified by either MALDI-TOF peptide mass mapping or MALDI-TOF/TOF peptide sequence analysis.

No.	Accession no.	Protein name	pI	MW	Match. Peptides	Coverage (%)	Score	MS p-value	MS/MS p-value	DM1/Normal ^d	p-value	Matched peptides ^e	Subcellular location	Function
457	O00170	AH receptor-interacting protein	6.09	38096	6/25	26%	58/56	0.034	N.A.	-1.42	N.A.	LPVWETIVCTMR; AKAVPLIHQEGNR	Cytoplasm	Signal transduction
440	P04217	Alpha-1B-glycoprotein	5.58	54809	7/34	21%	83/56	0.0001	N.A.	-2.54	N.A.	HQFLLTGDTQGR; CLAPLEGAR	Secreted	Inflammatory response
844	Q9Y587	AP-4 complex subunit sigma-1	5.08	17165	4/13	35%	60/56	0.018	N.A.	-1.62	0.035	TLLETEVIK; SNEQCSFIEYK	Membrane	Protein trafficking
710	P02647	Apolipoprotein A-I	5.56	30759	7/26	20%	71/56	0.0018	N.A.	-1.55	0.011	AELQEGAR; AKPALEDLR	Secreted	Cholesterol transport
609	P02649	Apolipoprotein E	5.65	36246	4/9	16%	56/56	0.046	N.A.	1.69	N.A.	LQAEAFQAR; LAVYQAGAR	Secreted	Lipoprotein transport
297	P02749	Beta-2-glycoprotein 1 ^a	8.34	39584	1/1	4%	96/56	N.A.	5e-007	-2.07	0.015	(VCPFAGILENGAVR)	Secreted	Coagulation
632	P10909	Clusterin/apolipoprotein J ^a	5.89	53031	1/1	1%	63/56	N.A.	0.00047	-1.6	0.031	(RPHFFFPK)	Secreted	Apoptosis
848	Q96A19	Coiled-coil domain-containing protein 102A	5.44	62816	9/27	13%	66/56	0.0054	N.A.	1.46	0.026	QTASALDCDLR; LEGELSQWK	Secreted	Unknown
309	Q9P109	Core2-GlcNAc-transferase 3	8.48	53589	7/25	14%	62/56	0.014	N.A.	-4.57	0.0039	DAIMVER; LEEQQR	Golgi	Glycosylation
269	O60260	E3 ubiquitin-protein ligase parkin	6.71	53602	6/25	16%	62/56	0.014	N.A.	1.53	0.067	LRVQCSTCR; VCMGDHWFVDV	Cytoplasm	Protein degradation
184	P02671	Fibrinogen alpha chain ^c	5.7	95656	12/36	14%	63/56	0.01	N.A.	-1.5	0.31	NSLFYQK; QFTSSTSYNR	Secreted	Coagulation
176	P02671	Fibrinogen alpha chain ^{b,c}	5.7	95656	14/44	18%	65/56	0.0062	N.A.	-1.42	N.A.	CPSGCRMK(ICy3); GDSTFESK	Secreted	Coagulation
343	P02675	Fibrinogen beta chain ^c	8.54	56577	15/44	31%	83/56	0.00011	N.A.	-31.28	0.00098	QDGSVDFGR; DNDGWLTSDPR	Secreted	Coagulation
330	P02675	Fibrinogen beta chain ^c	8.54	56577	16/39	31%	93/56	1.1e-005	N.A.	-28.44	0.00018	QDGSVDFGR; DNDGWLTSDPR	Secreted	Coagulation
334	P02675	Fibrinogen beta chain ^c	8.54	56577	13/34	31%	84/56	8.3e-005	N.A.	-4.15	0.00036	QDGSVDFGR; EDGGGWYNR	Secreted	Coagulation
335	P02675	Fibrinogen beta chain ^c	8.54	56577	7/23	16%	57/56	0.042	N.A.	-2.9	0.00051	GSWYSMR; DNDGWLTSDPR	Secreted	Coagulation
131	P02675	Fibrinogen beta chain	8.54	56577	8/28	19%	65/56	0.0071	N.A.	1.52	N.A.	SILENLR; QDGSVDFGR	Secreted	Coagulation
447	P02679	Fibrinogen gamma chain	5.37	52106	9/29	24%	82/56	0.00014	N.A.	-6.31	0.034	TSEVKQLIK; VGPEADKYR	Secreted	Coagulation
618	P02679	Fibrinogen gamma chain	5.37	52106	6/23	14%	70/56	0.0022	N.A.	-1.5	0.055	DNCCILDER; VELEDWNGR	Secreted	Coagulation
170	Q9UK05	Growth/differentiation factor 2	6.03	47861	6/20	15%	57/56	0.045	N.A.	1.46	N.A.	NKLEVTVESHR; STTPASNIVR	Secreted	Growth regulation
842	P00738	Haptoglobin	6.13	45861	5/11	11%	62/56	0.014	N.A.	1.39	0.061	LPECEAVCGKPK; TEGDGVYTLNDKK	Secreted	Inflammatory response
501	P00738	Haptoglobin	6.13	45861	8/40	18%	64/56	0.0081	N.A.	1.68	N.A.	VTSIQDWVQK; GSPWQAK	Secreted	Inflammatory response

402	P02790	Hemopexin	6.55	52385	6/17	19%	64/56	0.0089	N.A.	-1.42	0.0055	FDPVVRGEVPPR; YYCFQGNQFLR	Secreted	Heme transport
736	P01834	Ig kappa chain C region	5.58	11773	4/16	48%	64/56	0.0072	N.A.	-1.36	0.14	TVAAPSVFIFPPSDEQLK; VYACEVTHQGLSSPVTK	Secreted	Immune response
644	Q6XPS3	PI-3,4,5-trisphosphate 3-phosphatase TPTE2	8.96	61457	7/20	19%	56/56	0.051	N.A.	-1.37	0.015	VYNLCSEK; VQVMEKK	ER	Signal transduction
1102	Q9HCY8	Protein S100-A14	5.16	11826	4/15	45%	60/56	0.021	N.A.	1.37	0.0087	ETLTPSELK; IANLGSCNDSK	Cytoplasm	Signal transduction; Ca regulation
496	P00734	Prothrombin ^b	5.64	71475	6/25	15%	63/56	0.01	N.A.	-16.63	N.A.	GQQYQGR;	Secreted	Coagulation
101	P02787	Serotransferrin	6.81	79280	22/38	29%	108/56	3.2e-007	N.A.	-1.42	N.A.	EGYYGYTGAFK; DSGFQMNQLR	Secreted	Iron transport; Cell
630	P02768	Serum albumin	5.92	71317	8/17	11%	69/56	0.0028	N.A.	1.32	0.011	LCTVATLR; DDNPNLPR	Secreted	Transport/ Hemostasis
520	P02768	Serum albumin	5.92	71317	11/36	18%	82/56	0.00013	N.A.	1.33	0.0021	FQNALLVR; CATESLVNR	Secreted	Transport/ Hemostasis
533	P02768	Serum albumin	5.92	71317	8/28	15%	59/56	0.024	N.A.	1.34	0.015	HPDYSVLLLLR; RHPDYSVLLLLR	Secreted	Transport/ Hemostasis
460	P02768	Serum albumin	5.92	71317	7/21	13%	59/56	0.026	N.A.	1.35	0.015	RHPDYSVLLLLR; HPDYSVLLLLR	Secreted	Transport/ Hemostasis
464	P02768	Serum albumin	5.92	71317	9/27	17%	83/56	0.00011	N.A.	1.39	0.0018	FGERAFK; HPDYSVLLLLR	Secreted	Transport/ Hemostasis
507	P02768	Serum albumin	5.92	71317	7/21	13%	71/56	0.0018	N.A.	1.43	0.0018	HPDYSVLLLLR; RHPDYSVLLLLR	Secreted	Transport/ Hemostasis
617	P02768	Serum albumin	5.92	71317	6/13	9%	67/56	0.0044	N.A.	1.43	0.0011	HPDYSVLLLLR; RHPDYSVLLLLR	Secreted	Transport/ Hemostasis
655	P02768	Serum albumin	5.92	71317	13/31	20%	63/56	0.0093	N.A.	1.43	0.017	LCTVATLR; DDNPNLPR	Secreted	Transport/ Hemostasis
484	P02768	Serum albumin	5.92	71317	8/14	15%	86/56	5.2e-005	N.A.	1.46	0.0027	HPDYSVLLLLR; RHPDYSVLLLLR	Secreted	Transport/ Hemostasis
112	P35610	Sterol O-acyltransferase 1	9.08	65205	6/19	8%	61/56	0.018	N.A.	1.57	0.0081	AHSFVRENVPR; WGYVAMK	ER	Lipoprotein assembly
616	Q8NBS9	Thioredoxin domain-containing protein	5.63	48283	6/15	12%	57/56	0.039	N.A.	-1.4	0.052	LQPTWNDLGDK; KEFPGLAGVK	ER	Redox regulation
955	P02766	Transthyretin	5.52	15991	4/6	25%	57/56	0.037	N.A.	1.9	0.019	GSPAINVAVHVFR; GSPAINVAVHVFRK	Secreted	Thyroxine transport
619	P62256	Ubiquitin-conjugating enzyme E2 H	4.55	20699	5/12	27%	60/56	0.023	N.A.	-1.31	0.00081	VRVDLPDK; MSSSPGK	Cytoplasm	Protein degradation

^a Proteins identified by MALDI-TOF/TOF.

^b Putative ICy dye labeled peptides identified by MALDI-TOF MS.

^c Proteins appearing more than once were identified as isoforms with different % coverage of analyzed peptides, matched peptide numbers, MOWSE scores, average fold-thiol reactivity alterations, t-test values and matched peptide sequences for each identified protein.

^d Average fold-thiol reactivity alterations of replicate samples run on different gels from DeCyder analysis show abundance ratios for type 1 diabetic plasma versus healthy donor's plasma. Proteins displaying an average fold-difference of 1.3-fold up or down regulation are listed in the Table. Functions were ascribed from the Swiss-Prot databases and literature searches.

^e In MS analysis, we listed top 2 score peptide sequences in the matched peptide column. In MS/MS analysis, we listed the MS/MS-sequenced peptide with bracket in the matched peptide column.

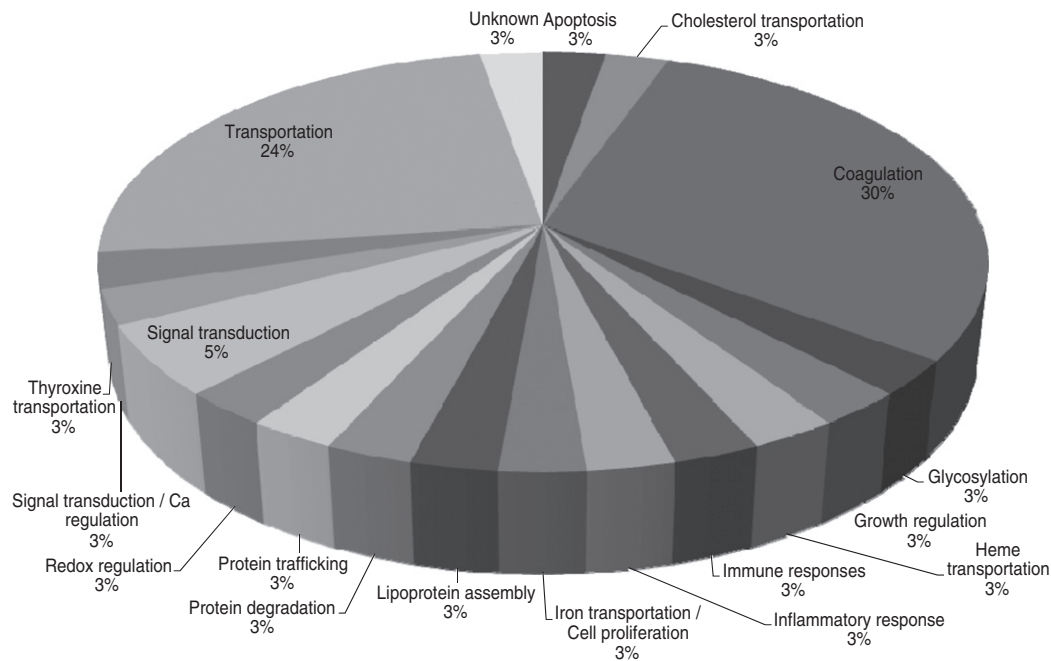


Fig. 9 – Percentage of plasma proteins identified from albumin and immunoglobulin G depleted plasma by 2D-DIGE/MALDI-TOF MS for type 1 diabetes mellitus according to their biological functions.

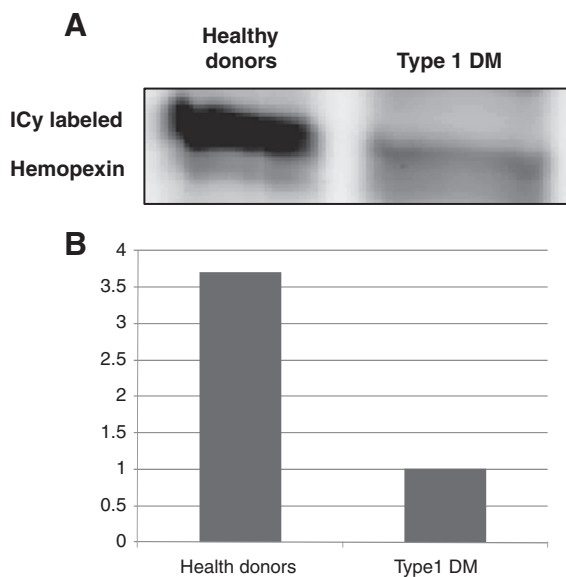


Fig. 10 – Validation of the thiol reactive plasma protein, hemopexin, identified through redox-proteomic study in between type 1 diabetes mellitus patients and healthy donors by immunoprecipitation. (A) ICy dye-labeled plasma samples from type 1 diabetes mellitus patients and healthy donors were immunoprecipitated with hemopexin antibody to confirm the alterations of thiol reactivity in hemopexin. The image was visualized by Ettan DIGE imager. (B) The thiol reactivities of hemopexin were normalized with hemopexin levels obtained from previous immunoblotting analysis to quantify the relative thiol reactivity alterations of hemopexin in type 1 diabetic plasma.

biomarkers which may associate with the progression and development of the disease. One of these putative markers, hemopexin, has been evidenced to be regulated by glucose concentration which is in turn mediated through a ROS-dependent mechanism in this study. The potential of utilizing these markers for screening and treating type 1 diabetes mellitus warrants further investigation.

Supplementary data related to this article can be found online at <http://dx.doi.org/10.1016/j.jprot.2012.04.047>.

Declaration of competing interests

The authors confirm that there are no conflicts of interest.

Acknowledgment

This study was supported by Chiayi Christian Hospital (grant R101-1) and also by the grants NSC 99-2314-B-705-002-MY2 and NSC 100-2311-B-007-005 of the National Science Council, Taiwan. Additionally, this work was also supported by Nano- and Micro-ElectroMechanical Systems-based Frontier Research on Cancer Mechanism, Diagnosis, and Treatment grant from National Tsing Hua University.

REFERENCES

- [1] Finne P, Reunanen A, Stenman S, Groop PH, Gronhagen-Riska C. Incidence of end-stage renal disease in patients with type 1 diabetes. *JAMA* 2005;294:1782-7.

- [2] Cameron JS. The discovery of diabetic nephropathy: from small print to centre stage. *J Nephrol* 2006;19(Suppl. 10): S75–87.
- [3] Merchant ML, Klein JB. Proteomic discovery of diabetic nephropathy biomarkers. *Adv Chronic Kidney Dis* 2010;17: 480–6.
- [4] D'Hertog W, Mathieu C, Overbergh L. Type 1 diabetes: entering the proteomic era. *Expert Rev Proteomics* 2006;3: 223–36.
- [5] Bang-Berthelsen CH, Pedersen L, Floyel T, Hagedorn PH, Gylvin T, Pociot F. Independent component and pathway-based analysis of miRNA-regulated gene expression in a model of type 1 diabetes. *BMC Genomics* 2011;12:97.
- [6] Reynier F, Pachot A, Paye M, Xu Q, Turrel-Davin F, Petit F, et al. Specific gene expression signature associated with development of autoimmune type-1 diabetes using whole-blood microarray analysis. *Genes Immun* 2010;11: 269–78.
- [7] Giacco F, Brownlee M. Oxidative stress and diabetic complications. *Circ Res* 2010;107:1058–70.
- [8] Vlassara H, Palace MR. Glycoxidation: the menace of diabetes and aging. *Mt Sinai J Med* 2003;70:232–41.
- [9] Nishikawa T, Edelstein D, Du XL, Yamagishi S, Matsumura T, Kaneda Y, et al. Normalizing mitochondrial superoxide production blocks three pathways of hyperglycaemic damage. *Nature* 2000;404:787–90.
- [10] Cumming RC, Andon NL, Haynes PA, Park M, Fischer WH, Schubert D. Protein disulfide bond formation in the cytoplasm during oxidative stress. *J Biol Chem* 2004;279:21749–58.
- [11] Timms JF, Cramer R. Difference gel electrophoresis. *Proteomics* 2008;8:4886–97.
- [12] Huang HL, Hsing HW, Lai TC, Chen YW, Lee TR, Chan HT, et al. Trypsin-induced proteome alteration during cell subculture in mammalian cells. *J Biomed Sci* 2010;17:36.
- [13] Lin CP, Chen YW, Liu WH, Chou HC, Chang YP, Lin ST, et al. Proteomic identification of plasma biomarkers in uterine leiomyoma. *Mol Biosyst* 2012;8:1136–45.
- [14] Chen YW, Liu JY, Lin ST, Li JM, Huang SH, Chen JY, et al. Proteomics analysis of gemcitabine-induced drug resistance in pancreatic cancer cells. *Mol Biosyst* 2011;7:3065–74.
- [15] Chen YW, Chou HC, Lyu PC, Yin HS, Huang FL, Chang WS, et al. Mitochondrial proteomics analysis of tumorigenic and metastatic breast cancer markers. *Funct Integr Genomics* 2011;11:225–9.
- [16] Chou HC, Chen YW, Lee TR, Wu FS, Chan HT, Lyu PC, et al. Proteomics study of oxidative stress and Src kinase inhibition in H9C2 cardiomyocytes: a cell model of heart ischemia reperfusion injury and treatment. *Free Radic Biol Med* 2010;49:96–108.
- [17] Gharbi S, Gaffney P, Yang A, Zvelebil MJ, Cramer R, Waterfield MD, et al. Evaluation of two-dimensional differential gel electrophoresis for proteomic expression analysis of a model breast cancer cell system. *Mol Cell Proteomics* 2002;1:91–8.
- [18] Hung PH, Chen YW, Cheng KC, Chou HC, Lyu PC, Lu YC, et al. Plasma proteomic analysis of the critical limb ischemia markers in diabetic patients with hemodialysis. *Mol Biosyst* 2011;7:1990–8.
- [19] Chan HL, Gaffney PR, Waterfield MD, Anderle H, Peter MH, Schwarz HP, et al. Proteomic analysis of UV-C irradiation-induced damage of plasma proteins: serum amyloid P component as a major target of photolysis. *FEBS Lett* 2006;580:3229–36.
- [20] Chan HL, Gharbi S, Gaffney PR, Cramer R, Waterfield MD, Timms JF. Proteomic analysis of redox- and ErbB2-dependent changes in mammary luminal epithelial cells using cysteine- and lysine-labelling two-dimensional difference gel electrophoresis. *Proteomics* 2005;5:2908–26.
- [21] Candiloros H, Muller S, Zeghari N, Donner M, Drouin P, Ziegler O. Decreased erythrocyte membrane fluidity in poorly controlled IDDM. Influence of ketone bodies. *Diabetes Care* 1995;18:549–51.
- [22] Saydah SH, Miret M, Sung J, Varas C, Gause D, Brancati FL. Postchallenge hyperglycemia and mortality in a national sample of U.S. adults. *Diabetes Care* 2001;24:1397–402.
- [23] Jouven X, Lemaitre RN, Rea TD, Sotoodehnia N, Empana JP, Siscovick DS. Diabetes, glucose level, and risk of sudden cardiac death. *Eur Heart J* 2005;26:2142–7.
- [24] Cai L, Li W, Wang G, Guo L, Jiang Y, Kang YJ. Hyperglycemia-induced apoptosis in mouse myocardium: mitochondrial cytochrome C-mediated caspase-3 activation pathway. *Diabetes* 2002;51:1938–48.
- [25] Chan HT, Lee TR, Huang SH, Lee HY, Sang TK, Chan HL. Proteomic analysis of a drosophila IBMPPD model reveals potential pathogenic mechanisms. *Mol Biosyst* 2012;8: 1730–41.
- [26] Lai TC, Chou HC, Chen YW, Lee TR, Chan HT, Shen HH, et al. Secretomic and proteomic analysis of potential breast cancer markers by two-dimensional differential gel electrophoresis. *J Proteome Res* 2010;9:1302–22.
- [27] Wu CL, Chou HC, Cheng CS, Li JM, Lin ST, Chen YW, et al. Proteomic analysis of UVB-induced protein expression- and redox-dependent changes in skin fibroblasts using lysine- and cysteine-labeling two-dimensional difference gel electrophoresis. *J Proteomics* 2012;75:1991–2014.
- [28] Tolosano E, Altruda F. Hemopexin: structure, function, and regulation. *DNA Cell Biol* 2002;21:297–306.
- [29] Mohanty P, Hamouda W, Garg R, Aljada A, Ghanim H, Dandona P. Glucose challenge stimulates reactive oxygen species (ROS) generation by leucocytes. *J Clin Endocrinol Metab* 2000;85:2970–3.
- [30] Wolff SP, Jiang ZY, Hunt JV. Protein glycation and oxidative stress in diabetes mellitus and ageing. *Free Radic Biol Med* 1991;10:339–52.
- [31] Chou HC, Lu YC, Cheng CS, Chen YW, Lyu PC, Lin CW, et al. Proteomic and redox-proteomic analysis of berberine-induced cytotoxicity in breast cancer cells. *J Proteomics* in press, (doi:10.1016/j.jprot.2012.03.010).
- [32] Targher G, Chonchol M, Zoppini G, Franchini M. Hemostatic disorders in type 1 diabetes mellitus. *Semin Thromb Hemost* 2011;37:58–65.
- [33] Rader DJ. Regulation of reverse cholesterol transport and clinical implications. *Am J Cardiol* 2003;92:42J–9J.
- [34] Rohrer L, Hersberger M, von Eckardstein A. High density lipoproteins in the intersection of diabetes mellitus, inflammation and cardiovascular disease. *Curr Opin Lipidol* 2004;15:269–78.
- [35] Walldius G, Jungner I. The apoB/apoA-I ratio: a strong, new risk factor for cardiovascular disease and a target for lipid-lowering therapy—a review of the evidence. *J Intern Med* 2006;259:493–519.
- [36] Wang XH, Chen SF, Jin HM, Hu RM. Differential analyses of angiogenesis and expression of growth factors in micro- and macrovascular endothelial cells of type 2 diabetic rats. *Life Sci* 2009;84:240–9.
- [37] Abaci A, Oguzhan A, Kahraman S, Eryol NK, Unal S, Arinc H, et al. Effect of diabetes mellitus on formation of coronary collateral vessels. *Circulation* 1999;99:2239–42.
- [38] Toblli JE, Cao G, DeRosa G, Di Gennaro F, Forcada P. Angiotensin-converting enzyme inhibition and angiogenesis in myocardium of obese Zucker rats. *Am J Hypertens* 2004;17: 172–80.
- [39] Boodhwani M, Sodha NR, Mieno S, Xu SH, Feng J, Ramlawi B, et al. Functional, cellular, and molecular characterization of the angiogenic response to chronic myocardial ischemia in diabetes. *Circulation* 2007;116:131–7.
- [40] Hart AW, Baeza N, Apelqvist A, Edlund H. Attenuation of FGF signalling in mouse beta-cells leads to diabetes. *Nature* 2000;408:864–8.

- [41] Kimura H, Miyashita H, Suzuki Y, Kobayashi M, Watanabe K, Sonoda H, et al. Distinctive localization and opposed roles of vasohibin-1 and vasohibin-2 in the regulation of angiogenesis. *Blood* 2009;113:4810-8.
- [42] Smith A, Morgan WT. Hemopexin-mediated heme transport to the liver. *J Biol Chem* 1985;260:8325-9.
- [43] Madian AG, Myracle AD, Diaz-Maldonado N, Rochelle NS, Janle EM, Regnier FE. Differential carbonylation of proteins as a function of in vivo oxidative stress. *J Proteome Res* 2011;10:3959-72.
- [44] Frantikova V, Borvak J, Kluch I, Moravek L. Amino acid sequence of the N-terminal region of human hemopexin. *FEBS Lett* 1984;178:213-6.
- [45] Gillery P. Oxidative stress and protein glycation in diabetes mellitus. *Ann Biol Clin (Paris)* 2006;64:309-14.
- [46] Yan SF, Ramasamy R, Schmidt AM. Receptor for AGE (RAGE) and its ligands-cast into leading roles in diabetes and the inflammatory response. *J Mol Med (Berl)* 2009;87:235-47.
- [47] Boulanger E, Wautier JL, Dequiedt P, Schmidt AM. Glycation, glycoxidation and diabetes mellitus. *Nephrol Ther* 2006;2 (Suppl. 1):S8-S16.
- [48] Vlassara H. The AGE-receptor in the pathogenesis of diabetic complications. *Diabetes Metab Res Rev* 2001;17:436-43.
- [49] Zill H, Gunther R, Erbersdobler HF, Folsch UR, Faist V. RAGE expression and AGE-induced MAP kinase activation in Caco-2 cells. *Biochem Biophys Res Commun* 2001;288:1108-11.
- [50] Yang H, Jin X, Wai Kei LC, Yan SK. Review: oxidative stress and diabetes mellitus. *Clin Chem Lab Med* 2011.
- [51] Trougakos IP, Gonos ES. Regulation of clusterin/apolipoprotein J, a functional homologue to the small heat shock proteins, by oxidative stress in ageing and age-related diseases. *Free Radic Res* 2006;40:1324-34.
- [52] Kim JH, Kim JH, Jun HO, Yu YS, Min BH, Park KH, et al. Protective effect of clusterin from oxidative stress-induced apoptosis in human retinal pigment epithelial cells. *Invest Ophthalmol Vis Sci* 2010;51:561-6.
- [53] Kim JH, Kim JH, Yu YS, Min BH, Kim KW. Protective effect of clusterin on blood-retinal barrier breakdown in diabetic retinopathy. *Invest Ophthalmol Vis Sci* 2010;51:1659-65.
- [54] Kim JH, Yu YS, Kim JH, Kim KW, Min BH. The role of clusterin in in vitro ischemia of human retinal endothelial cells. *Curr Eye Res* 2007;32:693-8.